Marine Geology 361 (2015) 111–125

Contents lists available at ScienceDirect

Marine Geology

journal homepage: www.elsevier.com/locate/margeo

Late Pleistocene and Holocene sea-level change and coastal paleoenvironment evolution along the Iranian Caspian shore

A.A. Kakroodi [a,*], S.A.G. Leroy [b], S.B. Kroonenberg [c], H.A.K. Lahijani [d], H. Alimohammadian [e], I. Boomer [f], A. Goorabi [a]

[a] Faculty of Geography, Department of Remote Sensing and GIS, University of Tehran, Iran
[b] Institute for the Environment, Brunel University, London, Uxbridge, UB8 3PH, London, UK
[c] Faculty of Civil Engineering and Geosciences, Department of Geotechnology, Delft University of Technology, The Netherlands
[d] Iranian National Institute for Oceanography (INIO), No. 3, Etamadzadeh St., Fatemi Avenue., Tehran 1411813389, Iran
[e] Geological Survey of Iran, Tehran, Iran
[f] School of Geography, Earth & Environmental Sciences, University of Birmingham, Edgbaston, Birmingham B15 2TT, UK

ARTICLE INFO

Article history:
Received 3 September 2014
Received in revised form 28 December 2014
Accepted 30 December 2014
Available online 8 January 2015

Keywords:
Caspian Sea
Rapid sea-level change
Diatom
Pollen
Holocene sea-level change

ABSTRACT

The level of the Caspian Sea is influenced by rivers mostly from the high latitudes of the Northern hemisphere and therefore any change of its catchments including temperature and precipitation directly reflects on Caspian Sea-level.

We reconstructed Late Pleistocene to Holocene Caspian Sea-level by a multi-disciplinary approach from a 27.7 m long core in the SE corner of the Iranian Caspian coast in the Gomishan Lagoon. Late Pleistocene deposits containing typical Pleistocene fauna and dated around 20,120 cal yr BP bordered with a major hiatus indicating sea-level fall. Lagoonal deposits with shells dated at around 10,590 cal yr BP suggest that, after this deep lowstand, an initial transgression started, leading to landward advance of barrier–lagoon systems which still continued without any lowstand until 8400 cal yr BP. This corresponded to a biofacies change from lagoonal to the deeper biofacies including diatom and Gastropoda species. Around 8400 cal yr BP sea-level started to fall again, and reddish oxidized sediments with abundant foraminifera (*Ammonia beccarii*) record a regressive phase around 7700 cal yr BP. The mid-Holocene between 15.7 and 4.9 depths is characterized by a shallow marine environment mostly with high carbonate and gypsum contents, and lagoonal and highstand tract with no subaerial facies. The upper part of the core above a 4.9 m depth reflects at least five Late Holocene Caspian Sea-level cycles from 3260 cal yr BP onward. The Caspian Sea-levels are influenced both by global and regional events.

1. Introduction

Studying past sea-levels brings information to understand future changes. The average rate of sea-level change in the oceans obtained from tide gauge over the last 50 yrs is $+1.8 \pm 0.3$ mm yr^{-1} (Nerem et al., 2006; Church et al., 2013). However the Caspian Sea (CS) has experienced much more rapid sea-level changes than the oceans: even in the 20t h century sea-level has fluctuated about 3 m, with a maximum rate of sea-level rise in the 1980s of up to 34 cm/yr, a hundred times faster than eustatic sea-level rise in the oceans (Kakroodi, 2012). The Caspian Sea (CS) (Fig. 1a) has experienced many cycles and exhibits a good example of short- and long-term changes of water level since the Late Pleistocene (Mansimov and Aliyev, 1994; Kaplin and Selivanov, 1995; Hoogendoorn et al., 2005; Kroonenberg et al., 2007; Kakroodi et al., 2012; Kazancı and Gulbabazadeh., 2013).

Therefore the CS is a laboratory with an ongoing rapid experiment of sea-level changes that allows us to study, for example, the impact of sea-level changes on coastal geomorphology, water quality, biota response, vegetation adjustment; hence the CS is potentially a source of information to any scientist interested in understanding the impact of future sea-level changes related to Global Climatic Change. Many previous sea-level curves have been produced for the CS, but often different from each other (see Varushchenko et al., 1987 for older data, furthermore Rychagov, 1977, 1997; Rodionov, 1994; Kroonenberg et al., 2007, 2008; Hoogendoorn et al., 2010; Kakroodi et al., 2012). Sheltered coastal environments commonly preserve thick sequences of Holocene sediments, offering an opportunity to investigate past climate, sea-level and land-level changes, as well as more local environment changes (Lamb et al., 2006). The south-east coast of the CS has low onshore and offshore gradients, that make it very sensitive to sea-level changes and is therefore an ideal place to obtain a record of past sea-level changes

The Southern Caspian Basin contains some of thickest sediment accumulation known on Earth, up to 22 km in thickness with deposits

* Corresponding author. Tel.:+98 9192119871.
E-mail address: a.a.kakroodi@ut.ac.ir (A.A. Kakroodi).

http://dx.doi.org/10.1016/j.margeo.2014.12.007

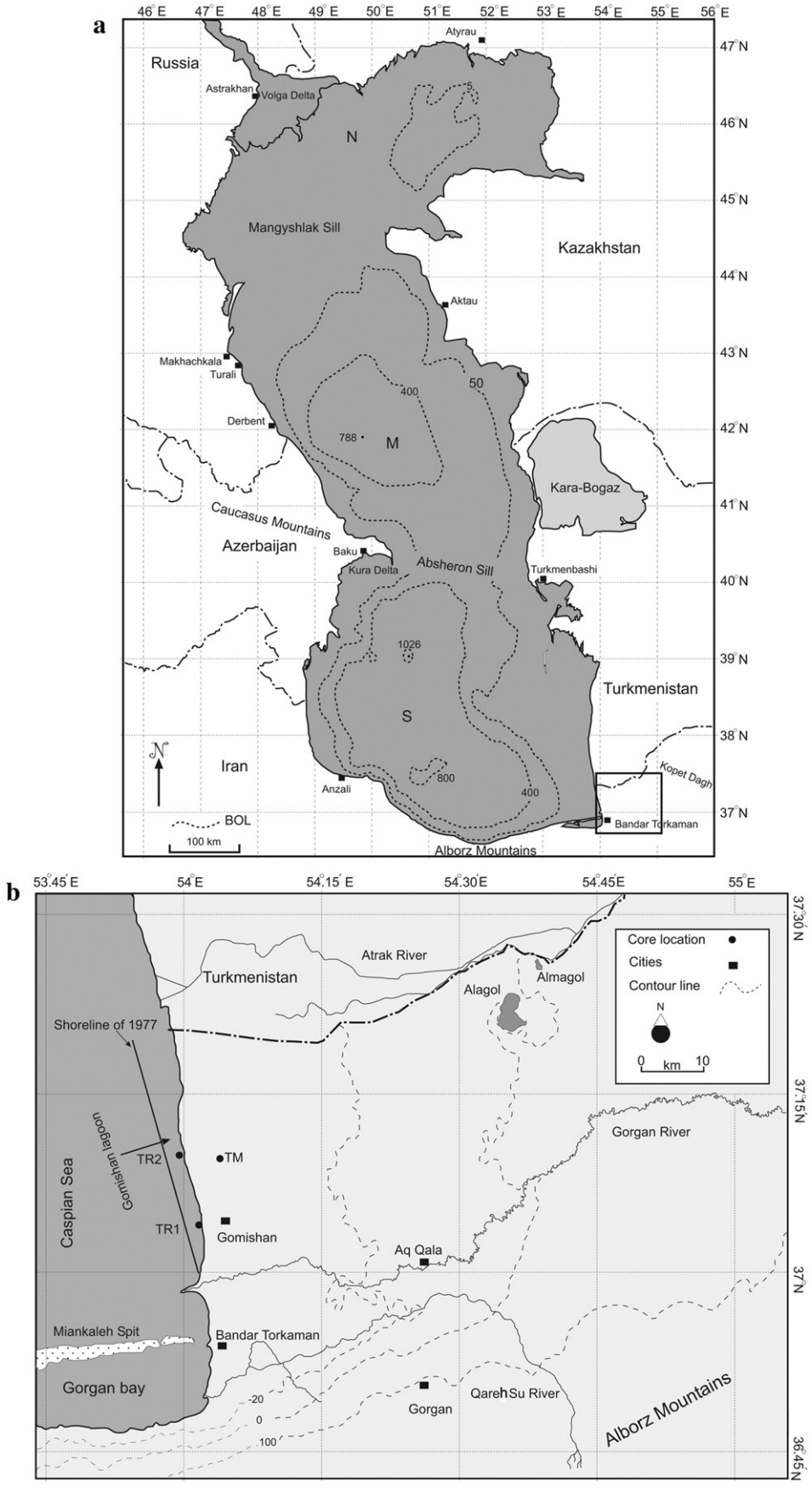

Fig. 1. The box shows the study area (a). Image b shows the recent coastal morphology derived from ETM image in 2001 and field data. Dotted lines indicate three contour lines, 100, 0, and −20 m extracted from SRTM data (b). It also shows the three basins of the CS based on the bathymetry including the Northern (N), Middle (M), and Southern (S) parts.

dating back as far as the Jurassic (Jackson et al., 2002). The South Caspian Basin is rapidly subsiding since 5.5 Ma at a rate of 0.44 mm yr^{-1} (Allen et al., 2002), or even 2.5 mm yr^{-1} (Inan et al., 1997).

Since its isolation in the Miocene, the CS has experienced rapid changes in sea-level over a timescale ranging from the secular, to the millennial, to glacial (Kaplin and Selivanov, 1995; Kroonenberg et al., 1997). During the Quaternary period, large ice-sheets extended into mainland Russia and blocked north-flowing rivers, which reversed their previous northward outlets to lower latitude lakes such as the Caspian Sea Basin (Mangerud et al., 2004). Recent paleo-channel studies in the Volga basin also reveal evidence of high surface runoff and higher inflow to the CS in Late Glacial times (Sidorchuk et al., 2009). It is not yet clear which of these two phenomena is responsible for the Late Pleistocene–Late Khvalynian highstand, which reached up to 50 m above oceanic level (Kroonenberg et al., 1997; Rychagov, 1997; Svitoch, 2009; Dolukhanov et al., 2010). The precise timing of this period is ambiguous due to different reservoir age corrections, reports of uncalibrated dates and reworked samples.

The CS experienced a deep regression in the early Holocene, called the Mangyshlak lowstand, reaching down to 113 m below oceanic level (BOL) (Kroonenberg et al., 2000) and also experienced several highstands up to 22 m BOL in the late Holocene (Kakroodi et al., 2012). The first Holocene sea-level curve for the CS was reconstructed by using outcrops in marine terraces and barrier deposits in Dagestan (Rychagov, 1977, 1997; Fig. 2). Fluctuations in CS sea-level have been studied in shallow and deep marine deposits focusing on different methods such as magnetic and geochemical (Chalié et al., 1997), paleoecological (Boomer et al., 2005) and palynological analyses (Leroy et al., 2007). However there is still no consensus so far for the precise timing of the fluctuations due to questionable sampling strategies and obsolete dating methods (Svitoch et al., 2006; Kroonenberg et al., 2007).

In the twentieth century, the CS experienced a full sea-level cycle with an amplitude of ±3 m between 1929 and 1995, showing sea-level rise between 1977 and 1995. A water level of about 26 m BOL was registered during most of the nineteenth century until 1930 but it then rapidly dropped, reaching a level of 29.4 m BOL in 1977, corresponding to the lowest level recorded over the previous 400 yrs (Rychagov, 1997). When the Caspian Sea-level (CSL) started to fall from 1929 to 1977, the newly reclaimed land along the coast was extensively used, so that extreme damage occurred to the newly built infrastructure and habitations (Kakroodi et al., 2014a,b) when sea-level unexpectedly started to rise almost 3 m from 1977 to 1995 (Fig. 3a). Satellite data indicate that CSL (Fig. 3b) has been relatively stable since 1995 with a falling trend from 2011 onwards as a result of a drought in Russia in 2010 (Arpe et al., 2012).

This paper focuses on: (1) Late Pleistocene and Holocene sea-level change and coastal evolution, and (2) how different biota respond to sea-level changes.

2. Study area

The Iranian coast in the southeast corner of the Caspian Sea, the Gomishan area, is characterized by a very gentle slope both onshore and offshore. It is very vulnerable to sea-level fluctuations (Kakroodi et al., 2012).

The main sources of sediment for the south-eastern Caspian coast are the Gorgan and Qare Su rivers draining the Alborz Mountains, and the Atrak River draining the Kopet Dagh Mountains (Fig. 1a, b). The Gorgan River provides the most sediment supply and its annual sediment load is around 1.336 million ton (Mister, 2001). The Gorgan River has formed a cuspate delta, which has constantly changed its course during the Holocene (Kakroodi et al., 2012). Further north, largely in neighboring Turkmenistan, a presently inactive branch of the Amu-Darya River, the Uzboy River, formed an important delta, which ceased developing in the 16th century (Boomer et al., 2000; Leroy et al., 2006 and 2007).

A second source of sediment is aeolian. The Southern Caspian lowland of Iran is part of the Eurasian loess belt stretching from northwestern Europe to Central Asia and China (Frechen et al., 2009). During the Pleistocene glaciations, northern Iran was an extensive area of increased dust accumulation and loess formation. These sediments are widespread and appear mostly on the northern foothills of the Alborz

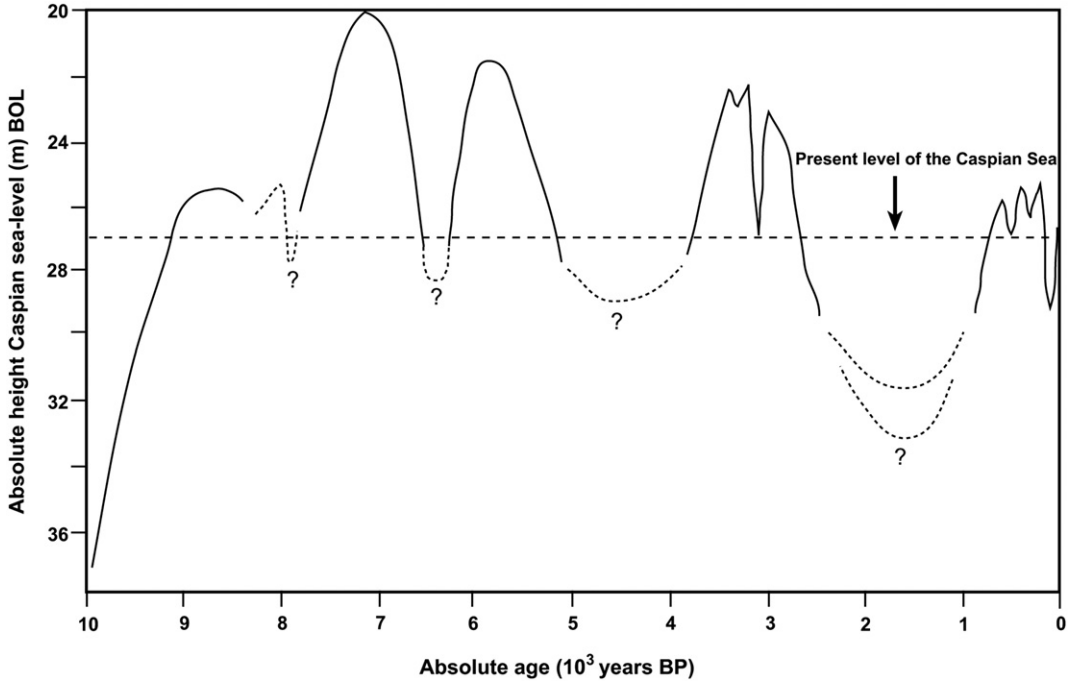

Fig. 2. Holocene sea-level curve of the Caspian Sea according to Rychagov (1977, 1997). Most lowstands in Rychagov's curve are not well defined. Ages are uncalibrated.

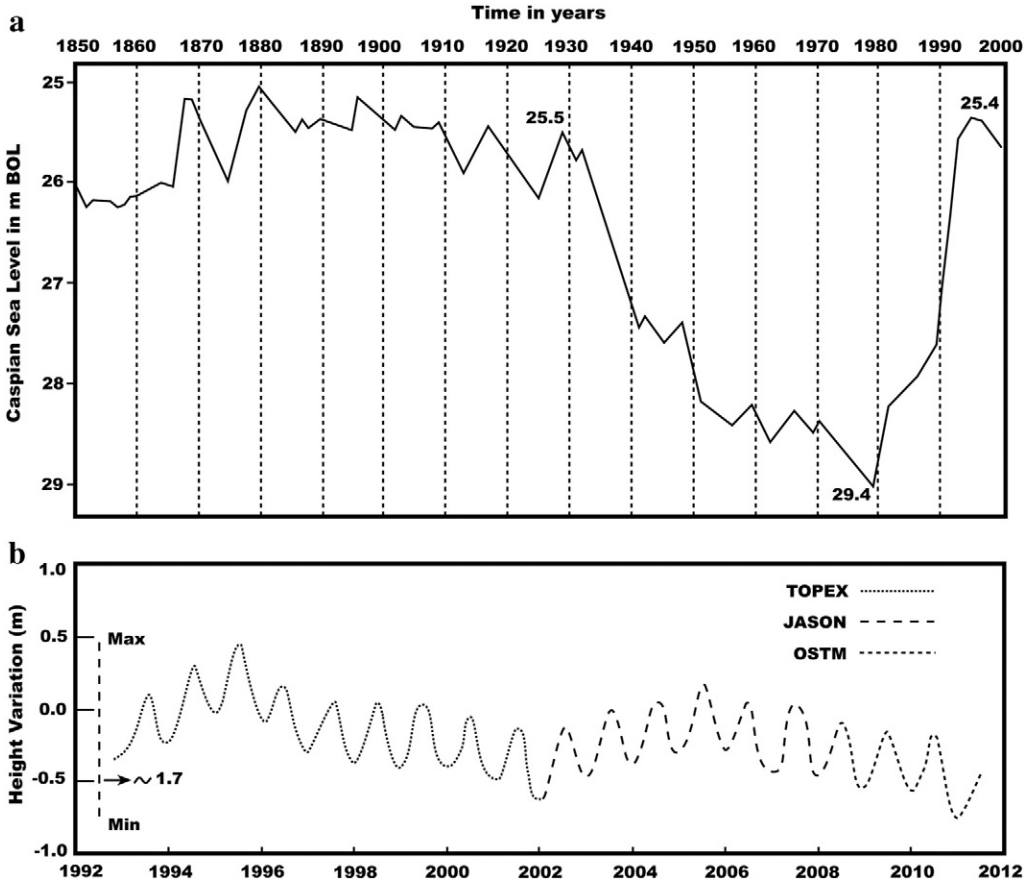

Fig. 3. The Caspian Sea curve since 1850 based on tide gauge data (source: National Iranian Oil Company compiled by: A. Jafari). Note the last cycle of Caspian Sea-level between 1929 and 1995 (a); and recent records of CSL from altimetry satellite data (http://www.pecad.fas.usda.gov/cropexplorer/global_reservoir/gr_regional_chart.cfm?regionid=metu&region=&reservoir_name=Caspian) (b).

Mountains and river incisions cut in the plains (Kazancı et al., 2004; Frechen et al., 2009).

The south-eastern corner of the CS is characterized by two prominent lagoons, the Gorgan Bay and the Gomishan Lagoon (Fig. 1b), each separated from the sea by a spit or barrier. The relatively deep Gorgan Bay along the north-facing part of the coast formed behind the prominent Miankaleh Spit, and is a product of strong west to east longshore sand transport. This lagoon survived the recent 20th century sea-level cycle (Kakroodi et al., 2012). The shallow south–north oriented Gomishan Lagoon formed along the west-facing part of the coast as a result of the landward movement of a narrow barrier due to rapid sea-level rise after 1977.

Two older lagoons dried out in the Gomishan area during rapid sea-level fall between 1929 and 1977 (Kakroodi et al., 2012). CSL rose rapidly back to its former highstand level in 1995, in the course of which the present-day lagoon (Gomishan Lagoon) formed at a lower part of the coast than the previous ones. Therefore the Gomishan coast presents one of the best locations for studying sea-level changes in the Caspian Sea (Kakroodi et al., 2012).

Lagoonal deposits are particularly important sea-level indicators, because lagoons form behind barriers during rapid sea-level rise, and may disappear by desiccation and silting up during rapid sea-level fall (Kroonenberg et al., 2000; Kakroodi et al., 2012). Therefore, the transgressive tract of the CS, as a whole, can often be identified in the local features of lagoonal facies. This facies is recorded by dark clayey deposits, rich in marine and brackish fauna. It also constitutes an excellent autochthonous sedimentary archive, undisturbed by waves and storm surges, which is useful for radiocarbon dating and also for conducting paleoecological work.

3. Material and methods

This study is on a 27.7 m long core (TM) drilled onshore in the south-eastern Caspian coast in 2009 with a coordinate position of 37° 09′ 56.48″ N and 54° 03′ 23.36″ E at around 2 m above present CSL (ca. −25.5 m BOL). Samples were taken at 60 cm intervals with plastic tubes (diameter 5.5 cm). A casing was used to prevent the hole from collapsing. In addition, two hand-pushed cores (TR1 and TR2 up to 100 cm long, diameter 3.5 cm) were collected in the modern lagoon to compare with the old lagoonal facies (Figs. 1, 4).

The cores were split and photographed. One half of each core was stored at the National Iranian Institute for Oceanography, while the other half was used for description, sampling and analysis. Sediment samples of on average 35 g were collected based on the sedimentary facies from the three cores. Samples were first dried in an oven at 55 °C, weighed and powdered to determine carbonate content (2 g) by using the Bernard calcimetric method (Lewis and McConchie, 1994). Organic matter (4 g) was measured by oxidation in hydrogen peroxide. Sub-samples (492) were extracted and washed by hydrogen peroxide solution (35%) for fully removing organic matter.

Finally, other sub-samples weighing 20 g were sieved through several mesh sieves (595, 250, 149, and 63 μm) to discriminate macroremains of Caspian Sea biota. Most adult and immature species of foraminifera (*Ammonia beccarii*, *Cornuspira* sp.) have been detected in 250 and 63 μm respectively. Adult *Elphidium* also have been found in the 149 μm fraction. Diatoms were only found in 63 μm and further analysis on the fraction less than 63 μm will be treated in another work. Based on salinity, Caspian Sea diatom flora consists of three different groups: marine, brackish and fresh (Karayeva and Makarova, 1973).

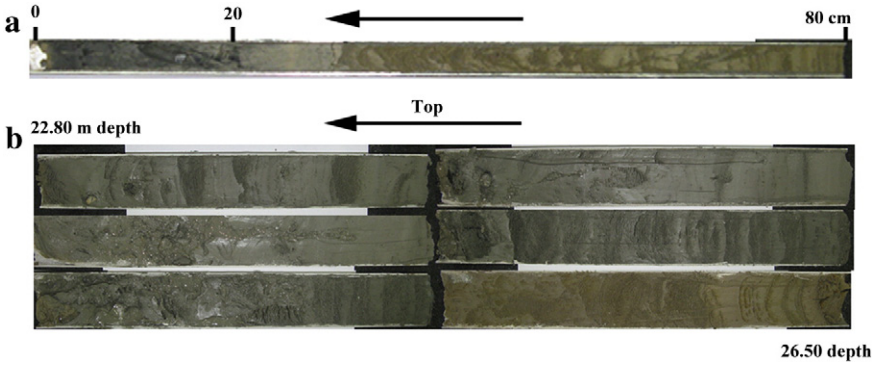

Fig. 4. Selected photographs of (a) recent sedimentary sequence with the presence of lagoonal facies (core TR 2) indicating highstand parasequence at the top of the core; and (b) TM onshore core between 26.5 and 22.80 m depths showing a deep regressive facies at the base (26 m depth) and transgressive facies at 25.7 m depth.

Charophyte gyrogonites and ichnofossils were only observed under a binocular microscope within the 60 μm fraction.

Charophytes (stoneworts) are a group of non-vascular, benthic macrophytes living entirely submerged in fresh water and brackish water; they never grow in marine environments with high salinity (Soulié-Märsche, 2008). The stoneworts have 10 species in the Caspian Sea. They develop mainly in the shallow water and their fossils are found in dark clayey silt and silty bays (Karpinsky, 2005). Charophytes can be useful as a salinity indicator. In the study area, *Lamprothamnium papulosum* is the most halo-tolerant taxa. Ichnofossils are geological traces of biological activity, which provides valuable information about paleoecology and paleoenvironment.

Quantitative analyses of Charophytes, ichnofossils and diatoms, identified under the binocular microscope, are expressed as number of specimens per gram and for diatoms as number of specimens per milligram. The identification of Caspian biota was done using various sources, among others: (1) Birshtein and Romanova (1968), (2) Tiffany and Britton (1952), (3) Hustedt (1930), (4) Boomer et al. (2005) for Ostracoda, and (5), Soulié-Märche (2008) for Charophytes.

Grain-size analysis for particles less than 63 μm was undertaken using a laser particle sizer (Fritsch Laser Particle Size Analyzer Analysette 22 Comfort) after decarbonating with "1N" hydrochloric acid. The samples are taken from the core separately and washed by hydrogen peroxide solution (2.5%) for radiocarbon dating and stable isotope measurements. High concentration of hydrogen peroxide may lead to dissolution or etching of the contaminate material (Ian Boomer, pers. comm., 2010). Isotope analyses were performed at the Stable Isotope Laboratory of the University of Birmingham on biogenic carbonate of Ostracoda (*Cyprideis*) that is the only genus that remains available throughout the whole core. 100–140 μg of ostracod bivalves were placed into 4 ml glass vials then sealed by a lid and pierceable septum. The vials were placed in a heated sample rack (90 °C) where the vial head space was replaced by pure helium via an automated needle system as part of a GV Instruments Multiflow preparation system. Samples were then manually injected with approximately 50 ul of phosphoric acid and left to react for 1 h before the headspace gas was sampled by needle and introduced into a continuous-flow GV Isoprime mass-spectrometer. Samples were calibrated using IAEA standards NBS-18 and NBS-19 and reported as ‰ on the VPDB scale. An external precision of better than 0.1‰ is typically achieved for both $\delta^{13}C$ and $\delta^{18}O$.

XRD and ICP-ES (0.5 g) analyses (24 samples) were made at the Ackme laboratory in Canada. A predetermined amount of sample was hand ground and then mixed with acetone to produce a thin slurry. The mixture was applied onto a glass slide which is scanned for determination by XRD.

For palynological analysis, the initial processing of the 43 core samples (1.5–2.5 ml in volume) involved the addition of sodium pyrophosphate to deflocculate the sediment. Samples were then treated with cold hydrochloric acid (10%) and cold hydrofluoric acid (32%), followed by a repeat HCl treatment. The residual fraction was then screened through 120 and 10 μm mesh sieves and mounted on slides in glycerol. Identification of the dinocysts is based on Marret et al. (2004), Leroy et al. (2010), Mudie et al. (2011) and Mertens et al. (2009). The number of pollen and spores counted was usually around 350. *Lycopodium* tablets were added at the beginning of the process for concentration estimates in the core samples only.

Pollen percentages were calculated on the terrestrial sum (excluding aquatic, spores, unknown or unidentifiable pollen, and non-pollen palynomorphs). The diagrams were plotted with psimpoll4 (Bennett, 2007). A zonation by cluster analysis (CONISS), after square root transformation, was applied. The zonation, based only on terrestrial taxa, was calculated for the percentage diagrams.

Dinocysts were counted at the same time as pollen and other microfossils. The total sum for dinocyst percentage calculations (mostly between 80 and 1800) is made of all dinocysts except *Brigantedinium* spp. The foraminiferal organic lining (a non-pollen palynomorph, or NPP, found in the palynological slides) was calculated in the same way as the *Brigantedinium* cysts.

4. Age–depth model

The chronology of the core is based on seven radiocarbon dates derived from shells (Table 1) which were identified under the binocular microscope and sorted in boxes. AMS ^{14}C analysis was carried out at the Raftar Radiocarbon Laboratory in New Zealand and at the radiocarbon laboratory of the Queen's University of Belfast. Reservoir age correction was applied, based on Kuzmin et al. (2007) considering a 390–440 reservoir effect and calibration followed with the marine dataset from Marine09 (Reimer et al., 2009). The ages cover the Late Pleistocene to Holocene time.

Sedimentation rates indicate a major hiatus between pre-Holocene and Holocene time (Fig. 5), which also corresponds to a biofacies change at a depth of 25.7 m (see below).

5. Sedimentary and biofacies record

The TM core was subdivided into eight lithological units with a subdivision of unit eight because of recent emergence of Hossien Gholi Bay (Figs. 4, 5, and 6), based on grain size, sedimentary structure, fossil content, color, carbonate and organic matter content, palynomorphs and geochemical data. They are discussed below from bottom to top. Some comments are also provided for the TR cores from the modern lagoon deposit.

5.1. Unit 1 (depth of 27.7–25.7 m) (Late Pleistocene)

This unit indicates two different facies, lower and upper deposits. At the base of the core, brownish to gray clayey silts are characterized by

Table. 1
AMS radiocarbon dating results for onshore TM core.

Sample ID	Depth (m)	Species	Lab ID	$\delta^{13}C$ [‰]	^{14}C age (BP)	Cal yr BP
No. 6 Top	2.5	Gastropoda	NZA34283	0.3	1497 ± 15	1139 to 948
No. 18 L.a.	8.9	Gastropoda: *Theodoxus*	NZA34285	2.5	3392 ± 15	3350 to 3160
No. 20 17 cm B	10.1	Ostracoda: *Cyprideis*	NZA34120	−4.7	3529 ± 25	3522 to 3320
No. 23	11.7	Gastropoda: *Theodoxus*	UBA-19908	−1.5	3644 ± 28	3633 to 3449
No. 31 10 cm Top	16.6	Foraminifera: *Ammonia beccarii*	NZA34427	0.6	7248 ± 50	7830 to 7590
No. 45 5 cm B	25.6	Gastropoda: *P. brusiniana*	NZA34121	3.1	9717 ± 45	10,700 to 10,470
No. 47 B	27	Ostracoda: *Cyprideis*	NZA34122	−0.4	17,367 ± 65	20,370 to 19,860

strong mottling and few marine fauna. It differs strikingly from the rest of the core. The lower part between 27.7 and 26 m depth is laminated and characterized by an alternation of mottled, highly oxidized reddish-brown silts and gray clayey silts.

The lower gray clayey silt between 27.7 and 26 m (25% clay) grades upwards to reddish-brown silt (92%) above 26 m depth. The XRD mineralogy at the 26.5 m depth shows significant quartz, moderate calcite, and minor albite, gypsum, halite, muscovite and clinochlore. The Geometric Mean Diameter (GMD) of sediment texture ranges from 15 μm at 27.6 m to 32 μm at the 25.9 m depth.

The upper part between the 26 and 25.7 m depths is more homogeneous and mottled. This unit of the core is characterized by an abundance of mica, large gypsum crystals (particularly above 26 m depth), and absence of foraminifera, diatoms, Charophytes (Fig. 6) and palynomorphs and the general scarcity of other fossils. Unit 1 ends in an erosional surface at a depth of 25.7 m (Fig. 5).

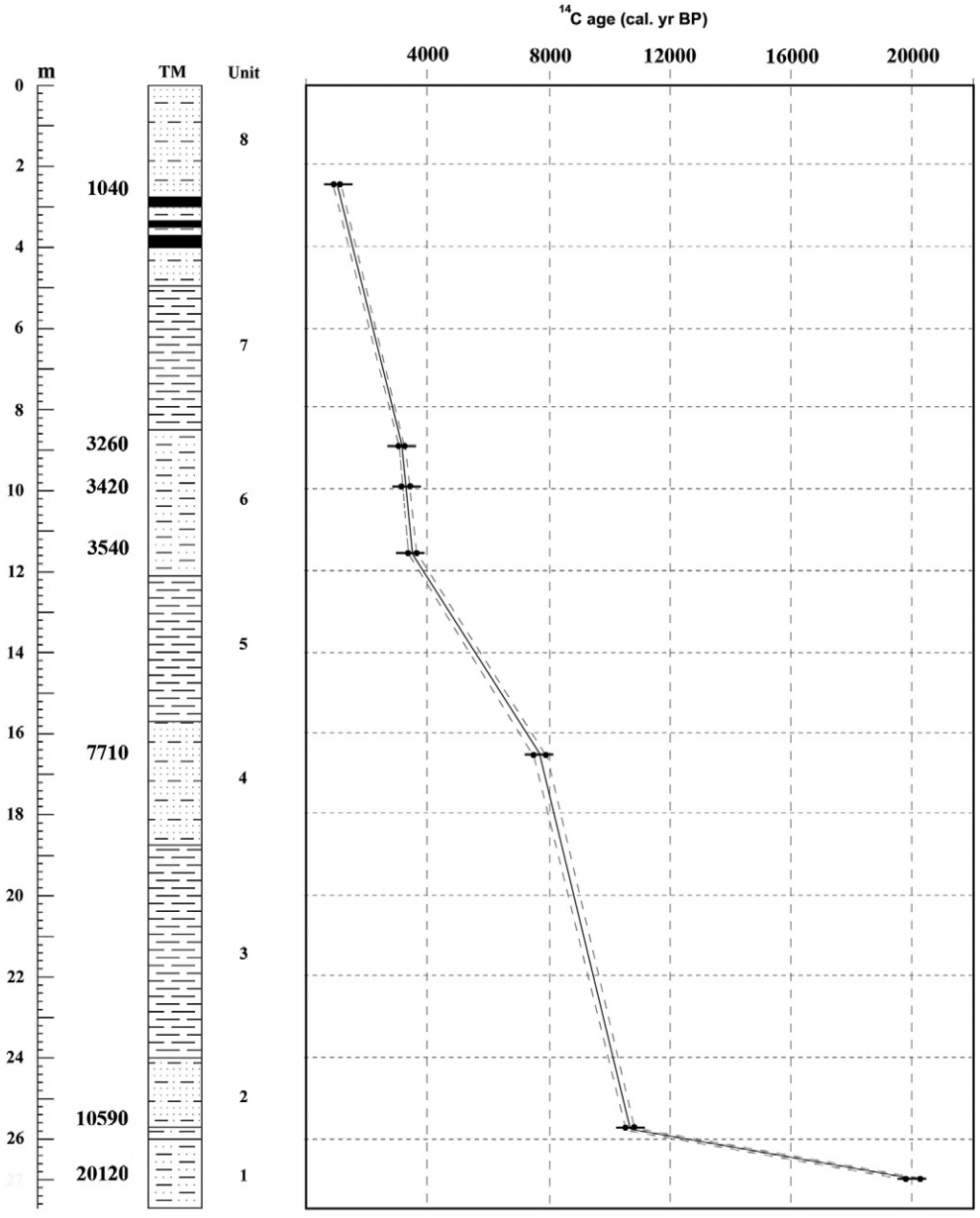

Fig. 5. Profile plot of calibrated dates associated with the lithology. Note the hiatus (horizontal gray line) between the Late Pleistocene and the Holocene.

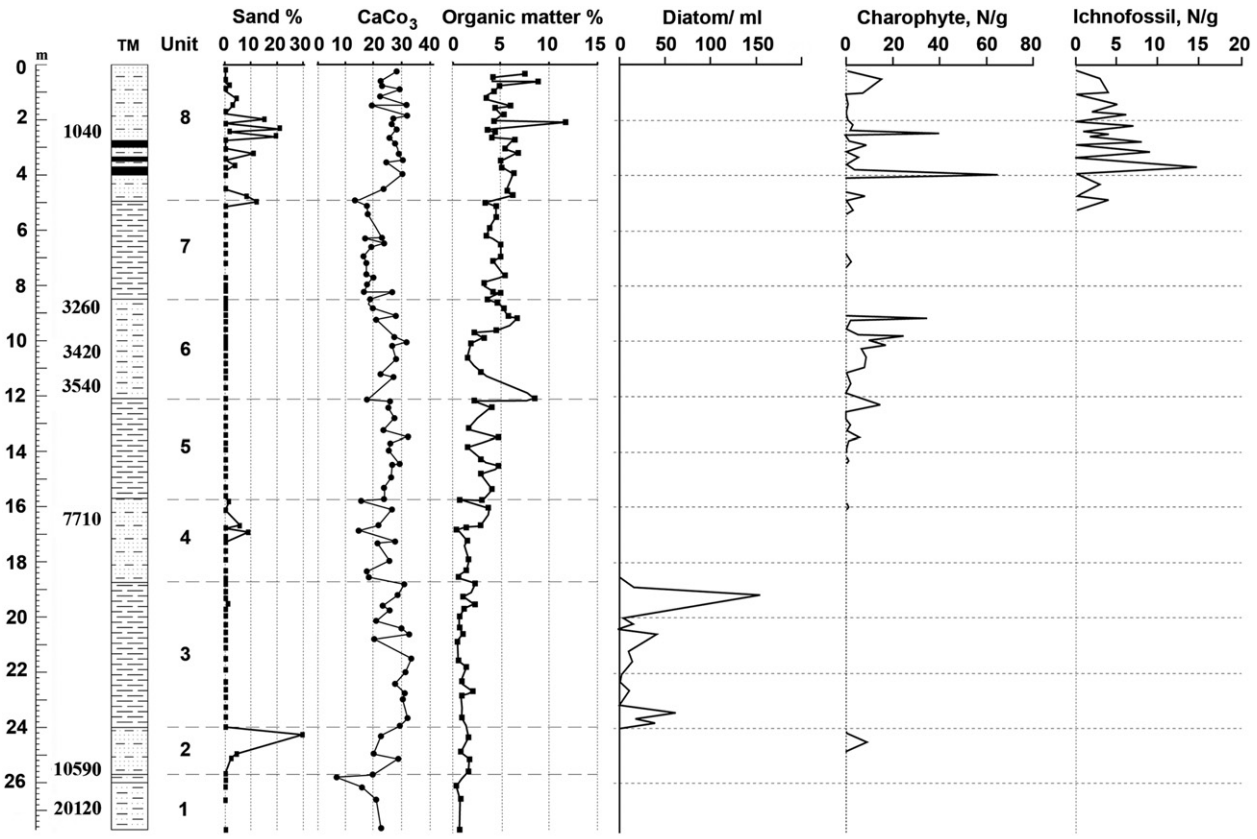

Fig. 6. Sedimentary units of micropaleontological data, abundance of the diatom (*Campylodiscus* sp.), Charophyte gyrogonites (*Lamprothamnium papulosum*) and ichnofossils (cases of Trichoptera).

The organic matter and carbonate content range between 0.33 and 1.3% and 8 and 21% showing the lowest values of organic matter and carbonate over the whole core.

Unit 1 shows a slightly negative $\delta^{18}O$ value (Fig. 7) than that of the modern value of 1.7‰ PDB, suggesting a fresher water environment.

This unit is characterized by Plio-Pleistocene ostracoda such as *Leptocythere bacuana*, *Caspiolla acronasuta*, *Bacuniella dorsoarcuata* and *Eucythere naphtatscholana* (Boomer et al., 2005) while most ostracods disappear in the uppermost reddish part. The lower part is at a depth of 27 dated on Ostracoda at 20,120 cal yr BP, which is shown in the stratigraphic profile (Fig. 6). This unit probably represents marine deposits that at the top were strongly oxidized during a subsequent regression.

5.2. Unit 2 (depth of 25.7–24 m) (Holocene)

Gray to dark clayey silt laminated with fine sand indicates a different sedimentary environment than the upper part of the previous unit (Fig. 4). Coarse silt (80%) passes upwards into silt and very fine sand (25%) with intercalated clay laminae. At above the 25 m depth of this unit, sandy silt thickness reaches 8 cm and the GMD of sediment texture shifts to 56 μm within the sandy silt. The sand content exceeds 25% of texture (Fig. 6).

X-ray diffraction of this unit presents a mineralogy similar to Unit 1 but it also contains minor dolomite with very minor gypsum.

Unit 2 also shows slightly more negative $\delta^{18}O$ values than the modern value of 1.7‰ PDB, suggesting a predominantly fresh water environment.

The carbonate and organic matter contents rise to 29 and 2% respectively, indicating increased productivity. The fauna is characterized by abundant Foraminifera and Ostracoda, mainly *Ammonia beccarii*, *Cyprideis* and also other fossils such as Gastropoda (*Theodoxus*), Bivalve (*Dreissena caspia*), as well as Charophytes.

The unit also contains wood and abundant seeds that mostly belong to the aquatic plants, *Zannichellia* and *Najas*. In this unit, the terrestrial pollen spectra are largely dominated by Amaranthaceae–Chenopodiaceae (A–C); the other herbs are *Artemisia* and Poaceae. Some tree pollens are present such as deciduous *Quercus*, and very low numbers of *Carpinus betulus* and *Alnus* (Fig. 8).

The reconstructed landscape is a semi-desert locally, with coastal salt marshes, and with some distant influence of more forested areas in the nearby Alborz Mountains. The large dominance of *Impagidinium caspienense*, a dinoflagellate cyst characteristic of brackish waters such as the modern day sea with of salinity 13‰, indicates an open water setting; however a coast with a lagoon cannot be far from the core location as pollen of the brackish aquatic plant, *Ruppia* is observed. At a depth of 25.6 m, a radiocarbon age of 10,590 cal yr BP was obtained on Gastropoda. On the basis of the sedimentological characteristics and paleoecological indicators this unit is thought to represent lagoonal deposits overlain by a thin layer of barrier sand.

5.3. Unit 3 (depth of 24–18.75 m)

This unit comprises alternating layers of dark gray clay (30%) and silt and the GMD of the sediment is finer than the unit 2, i.e., 9 μm. The interval between 20.80–20.30 m depths is characterized by a rapid alternation of light olive clayey silt rich in bivalves, particularly *Hipanis* sp., and dark olive clayey silt.

The XRD mineralogy at a depth of 23.6 m shows a subtly different mineralogy from the former unit with moderate quartz, moderate calcite, minor albite, halite, clinochlore, muscovite and the absence of gypsum. $\delta^{18}O$ values in Unit 3 become abruptly more negative and reached the minimum of the whole core (−5.5‰), suggesting an

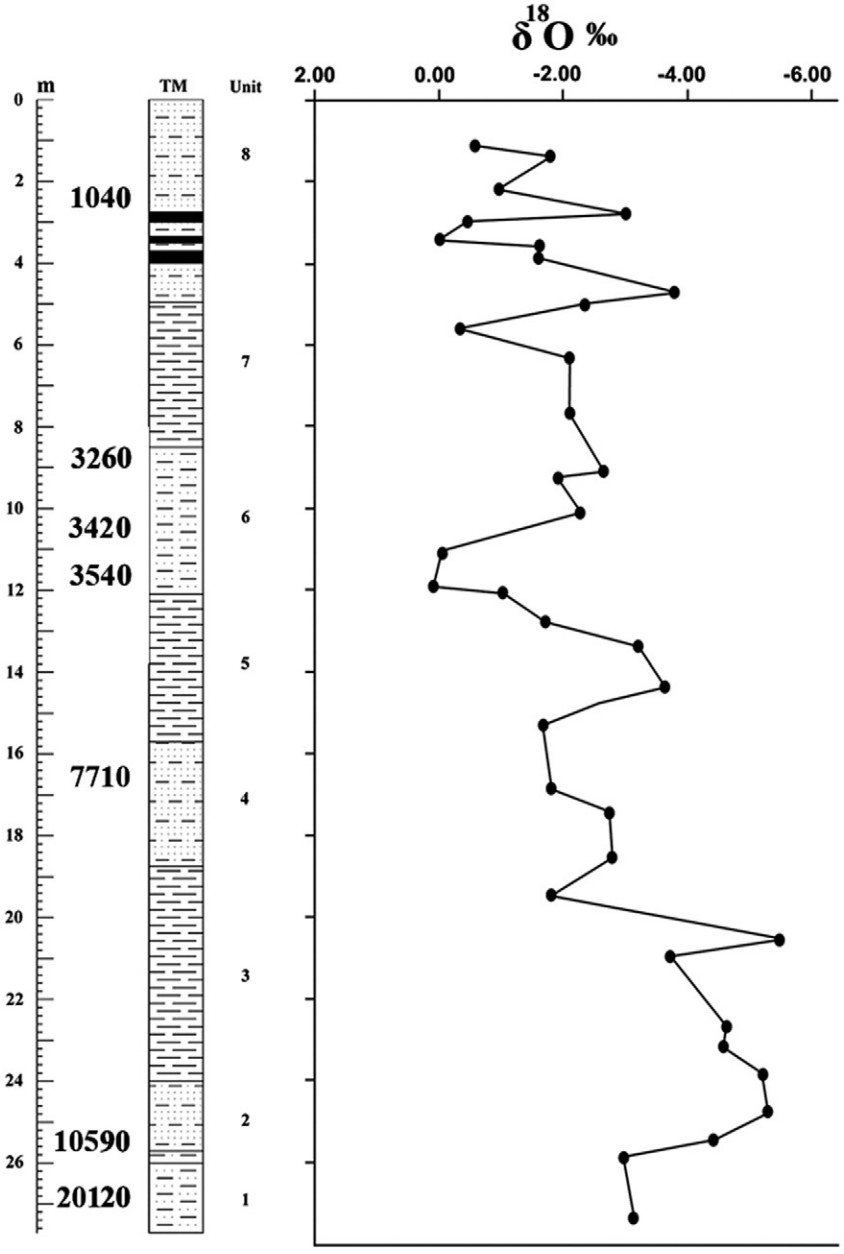

Fig. 7. Chronostratigraphy and xygen isotope curve associated with lithological units of core TM.

important extra influx of fresh water between 10,600 and 7700 cal yr BP, probably from the Volga (−12.9‰ PDB; Ferronsky et al., 2003), as this river provides more than 80% of the present annual flow, together with some smaller rivers. The carbonate and organic content varies between 21 and 34% and between 0.6 and 2% respectively.

The biofacies has the highest content of large diatoms in the whole core (Fig. 6), with especially high abundances of *Campylodiscus* sp. (*Clypeus*?) and, above 19 m depth, *Gyrsigma* sp. (*Kulzingii*?). The majority of the diatom fauna in this unit belongs to the brackish diatom, *Campylodiscus* sp. (*clypeus*?) and fresh-water diatom, *Gyrosigma* sp. (*kutzingii*?).

Gastropoda are equally abundant including assemblages with *Pyrgula* sp., and *Anisus*. The dark horizon between 20 and 18.8 m contains large diatoms and Gastropoda, mainly *Anisus*. It also contains a few *Ammonia beccarii* and *Cyprideis*, but no Charophytes.

At the beginning of this unit *Artemisia*, Asteraceae Liguliflorae and *Carpinus betulus* pollen percentages sharply increase, while in the second part, a peak of arboreal pollen is marked with maxima of deciduous *Quercus*, *C. betulus* and *Parrotia persica*, reflecting the extension of forest belts in the mountains towards the steppic plain and a vegetation optimum. In this unit, the most open and the deepest water of the sequence, with minimal continental influence, has been reconstructed (Fig. 8).

Therefore this unit appears to have been deposited in a low energy marine environment in a deeper part of the basin, although the oxygen isotope ratios are still close to fresh water values.

5.4. Unit 4 (depth of 18.75–15.7 m)

This unit is characterized by dark gray silt and silty clays and a sandy peak in the middle, with upwardly increasing mottling indicating oxidation. The GMD of sediment ranges from 16 μm at the base to 37 μm at the top. It shows upward coarsening with laminated silt and fine sand, ranging from 82.3% silt and 17.7% clay at the base to 88.3% silt, 8.3% clay and 3.4% sand at the top. The fine sand and coarse silt

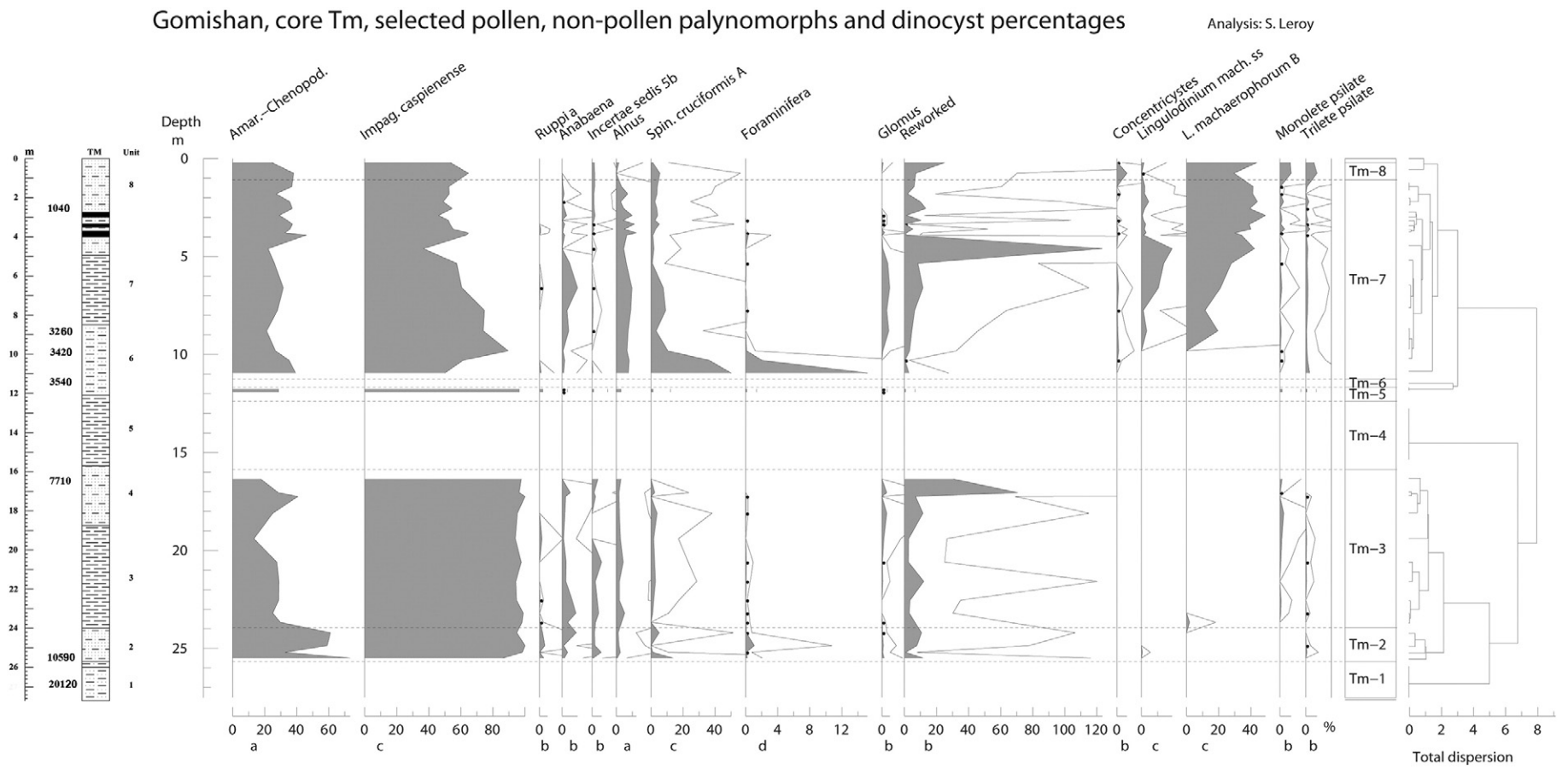

Fig. 8. Selected pollen, non-pollen palynomorphs and dinocysts from core TM, calculated in percentages. Analyses: Suzanne Leroy. The zonation by CONISS is based on terrestrial pollen taxa only. a: percentage of the sum of terrestrial pollen; b: percentage of the sum of terrestrial pollen, but not included in that sum; c: percentage of the sum of the dinocysts (excluding *Brigantedinium*); and d: percentage of the sum of the dinocysts (excluding *Brigantedinium*), but not included in that sum. The light lines are the 10 times exaggeration curve of the shaded lines. The continuous horizontal lines indicate the lithological units, the thin dashed horizontal lines are the pollen zones.

deposits are also rich in organic matter. The XRD mineralogy indicates significant quartz content at 18.1 m depth. Heavy minerals are mostly magnetite and hematite.

In Unit 4 a major increase in $\delta^{18}O$ values from −5.5 to −1.85‰ might indicate higher salinity or also higher temperatures. The carbonate content ranges between 15 and 28% and the organic matter content is at 0.6–4%. The biofacies includes bivalves, mostly *Dreissena polymorpha*, and further Gastropoda, Ostracoda, mainly *Leptocythere striatocostata*, large *Ammonia beccarii* and *Elphidium*, whereas the *Campylodiscus* sp. diatom strongly decreased (Fig. 6) with respect to the previous unit. At the base, the biofacies is characterized by Gastropoda, mostly *Pyrgula*, together with a large number of bivalves, mostly *Hypanis* sp.

The oxidized sandy silt facies at the top of this unit contains abundant *Ammonia beccarii*, which have been dated at 7710 cal yr BP.

The pollen concentration in this unit is low, with three samples out of four providing palynomorphs. Based on the arboreal pollen, the terrestrial environment is similar to the previous unit but slightly drier (slight increase of A–C and *Artemisia* pollen). The dinocysts and the NPPs still indicate a marine environment. This unit has been interpreted as shallow lagoonal deposits, which were subsequently exposed.

5.5. Unit 5 (depth of 15.7–12.10 m)

Unit 5 consists of homogeneous olive silt and clay, above 12.9 m depth showing mottling and intercalations of thin layers of evaporites (1.5 to 3.5 cm thickness). It consists of 83% silt and 17% clay at the base and 87.8% silt and 12.2% clay at the top. The GMD of texture differs from 17 to 18 μm respectively. X-ray diffraction of the evaporitic layer indicates gypsum, calcite and quartz. Unit 5 probably indicates increasing fresh water influence again, while at the 12.1 m depth it becomes less negative. Carbonate content ranges between 24 and 32%. The organic content varies between 2 and 5%.

Overall, the biota content is low, but tends to increase upwards. The biofacies is dominated by foraminifera and ostracods. It starts with few *Ammonia beccarii* and *Cyprideis* but includes a large number of *Cyprideis* and *A. beccarii* specimens at a depth of 14.8 m. At a depth of 12.80 m, there is a concentration of bivalves, mostly *Dreissena*, Gastropoda assemblages mainly *Anisus* (*Eichwaldi*, *Kolesnikovi*), Charophytes, and shell fragments which probably record a surge deposit. Unit 5 (pollen zones 4–6) is mostly devoid of palynomorphs.

The sedimentary record suggests shallow marine deposits. At the top, the facies is however characterized by mottling, large gypsum crystals, calcite and minor halite, and some bioactivity traces, pointing to temporary emergence under hypersaline conditions.

5.6. Unit 6 (depth of 12.10–8.50 m)

Unit 6 is composed of alternating laminated dark to gray clayey silts and more homogeneous olive clayey silts. The clay content reaches 39.6% within the dark clayey silt. The GMD of the dark clayey silts reached 17 μm while it ranged around 22 μm in the olive clayey silts. The carbonate content of the unit as a whole ranges between 18. 8 and 30.9%.

The dark clayey silts show relatively high content of organic matter up to 9% at 12.15 m depth, and the values remain high throughout, between 2 and 7%. The dark clayey silt deposits at the base of Unit 6 show $\delta^{18}O$ values around −1.73‰, close to modern values.

The dark clayey silt contains bivalves, mostly *Cerastoderma*, shell fragments, Gastropoda (mostly *Pyrgula and Theodoxus*) and Charophytes. It also contains ostracod assemblages, mainly *Cyprideis* and *Leptocythere*, as well as seeds of *Zannichellia*, *Najas* and some unidentified seeds.

From the base of this unit at 11.7 m depth within dark and gray silt, a radiocarbon date was obtained on Gastropoda at 3540 cal yr BP.

Two layers very rich in biota made of an assemblage of Ostracoda, bivalves, shell fragments, Gastropoda, Foraminifera and Charophytes, occur at 10.3 and 8.9 m depths. From these two layers radiocarbon dates at 3420 and 3260 cal yr BP have been obtained on Gastropoda.

The olive silts contain much lower abundance of biota. They contain numerous small gypsum “desert roses” dispersed among the olive clayey silts, which on inspection by XRD consist mainly of gypsum with quartz and calcite. Higher value of $\delta^{18}O$ value occurs in olive clayey silts (+0.8‰), probably representing hypersaline lagoonal conditions. Generally this unit shows a decrease of fresh water influence from base to top.

The bottom palynological sample (11.57 m depth) in this unit is sterile in palynomorphs; this is followed by a slow increase of the palynomorph concentration throughout this unit. The terrestrial environment is steppe but this time the coastal strip is covered by an Alder carr (wetland with alder trees). The distant influence of the forest is now marked by the presence of *Fagus* and *Pterocarya* pollen. Pollen of *Cerealia*-t. and *Plantago* are now frequent, reflecting possible human activity nearby (Behre, 1981). At 10.95 and 10.30 m depths, the non-pollen palynomorph assemblages contain high percentages of the low salinity *Spiniferites cruciformis* (salinity ≤7) and of foraminiferal linings. These values decrease sharply in the middle of the unit. In the last sample at 8.80 m, the beginning of the occurrence of *Lingulodinium machaerophorum* is felt. This unit presents therefore the signs of a rapid change in the environment from relatively fresh to brackish waters.

The dark silty clays may represent lagoonal facies, and the olive clayey silts shallow marine to hypersaline conditions.

5.7. Unit 7 (depth of 8.50–4.95 m)

Unit 7 consists of conformable dark to gray clay and silt and laminated silt, with mottling at the top. The GMD of texture shows 8.4 μm with a coefficient of variation of 0.6%. The amount of clay increases in this unit with respect to the previous unit and contains 41% at 6.40 m depth. XRD analysis shows abundant to significant quartz with moderate calcite, albite, muscovite, and minor halite and kaolinite.

Unit 7 shows $\delta^{18}O$ values between −2 and −3‰ PDB without much variation.

Unit 7 is characterized by high abundance of organic matter (5%), wood, and low carbonate content (16%).

The amount of fauna decreases relative to a dark and clay silt layer. The fauna consists mainly of fresh water fauna such as *Hypanis vitrea*. The fauna also contains a few Ostracoda, *Ammonia beccarii* and abundant *Cornuspira* sp. Some Coleoptera remains are found in this unit. Steppe still dominates the landscape as previously, with decreasing values of Poaceae and *Cerealia*-t. at the top of the unit. The percentages of *Impagidinium caspienense* drop to a minimum across this unit, while two forms of *Lingulodinium machaerophorum* sharply increase. Fungal spores are abundant, especially *Glomus*. The NPP, *Pseudoschizaea* is occasionally present. These last two taxa indicate soil washed into the lagoon by erosion on the nearby land.

Unit 7 is interpreted as shallow lagoonal environment strongly influenced by river input, judging from biofacies and sedimentological characteristics. The lack of marine flora such as diatom and scarcity of Charophytes and marine fauna also confirm this.

5.8. Unit 8 (depth of 4.95–0 m)

This unit includes two subunits which at the top encompasses old lagoonal deposits which emerged as a result of rapid sea-level fall between 1929 and 1977 (Kakroodi et al., 2012).

The sub-unit between 4.92–2.5 m is composed of an alternation of very brown to reddish fine sand and sandy silt layers with mottling and oxidation, and dark clayey silt layers (74% silt and 26% clay), each of which presents an erosional surface at the top (Fig. 6).

At least three dark clayey silt facies were identified, with thicknesses varying between 30 and 17 cm. The GMD of the dark silty clays is 6 μm. The XRD mineralogy at 3.9 m depth indicates moderate quartz, Mg-calcite, minor to moderate calcite, halite, minor albite, gypsum, muscovite and kaolinite or clinochlore. Other XRD analyses of these sediments also indicate a similar mineralogy but the amount of quartz changes from moderate to significant. The organic content ranges between 5 and 6%, whereas the carbonate content varies between 30 and 28%.

The dark clayey silt contains foraminifera (*Elphidiella brotzkajae*, *Cornuspira* sp., *Ammonia beccarii*), Charophytes (*Lamprothamnium papulosum*), Gastropoda (*Theodoxus pallasi*) as well as wood and seeds, mostly *Zannichellia*.

The brown to reddish fine sand and sandy silt layers with high mottling and oxidation vary in thickness between 13 and 23 cm. The GMD of sandy silt reaches 35 μm.

The XRD analysis shows significant quartz, minor to moderate Mg-calcite, calcite, minor halite, albite, gypsum muscovite and kaolinite. Unit 8 presents rapid variations between −2.98‰ in the dark clayey silts and −0.98‰ in the brown sandy silts, suggesting alternating fresh and brackish conditions.

This unit contains similar assemblages of fauna and macroflora as the dark clayey silt, but the most distinguishing components in the brown to reddish sandy silt and fine sand are abundant ichnofossils, about 1 cm long calcareous, dwelling structures, pointing to biological activity. The ichnofacies of the Late Holocene within the subaerial facies probably consists of the aquatic larva of insects such as Trichoptera. Here the tube is mostly made from calcite with a tube structure. Alternation of brown to reddish fine sand and sandy silt contains ichnofossil trace and disappears in lagoonal facies (dark clayey silt). The most abundant ichnofossils appeared at a depth of 4.5 m upwards within subaerial facies (Fig. 6). A radiocarbon age 1040 cal yr BP was obtained on Gastropoda at a depth of 2.5 m. The sedimentary record and biofacies indicate lagoon–barrier or spit environment throughout.

The upper subunit between 2.5–0 m is composed of brownish medium to very fine sand, clayey silt and laminated gray clay, mottled and highly oxidized facies. The GMD is 29 μm in brown clayey silt.

The high organic content in this sub-unit ranges between 3 and 12%, and carbonate content also varies between 20 and 32%, showing the maximum content of organic matter and high carbonate content respectively of the whole core.

The biofacies consists of bivalves, mostly *Cerastoderma*, shell fragments, foraminifera such as *Ammonia beccarii*, *Elphidiella brotzkajae* and *Cornuspira* sp., as well as Ostracoda, mostly *Cyprideis*. Lithologically Unit 8 encompasses the upper part of pollen zone 7, while the uppermost meter is a separate pollen zone (Tm-8). The pollen concentration, after reaching a peak at the beginning of Unit 8 (5.36–2.90 m depth), decreases sharply to the top, i.e., 0.20 m depth, while the dinocyst concentration increases (Fig. 8). The steppe is invaded by A–C, showing the development of a salt marsh probably where previously an Alder carr existed. Poaceae have minimal values, while *Cerealia*-t. pollen is absent. *Carpinus betulus* and *Pterocarya* values decrease; while at the top of pollen zone 8, some trees are planted as seen in the increasing percentages of *Quercus*, *Pinus* and perhaps *Acer*. This indicates a landscape profoundly modified by human activities. The values of *Impagidinium caspienense* are homogenously moderate across this unit, while the values of one of the two forms of *Lingulodinium machaerophorum*, from *ss* (i.e., sensu stricto) collapse and those of form B maintain maximal values (for identification of the various forms *L. machaerophorum*, see Marret et al. (2004) and Leroy et al. (2006)). The shorter spines of form B indicate a lower salinity as established by Mertens et al. (2009).

Fungal spores are still present but in lower percentage than the first part of pollen zone TM-7. Pseudoschizaea and Pteridophyte spores reach a maximum in the upper 75 cm (pollen zone Tm-8). This is interpreted as an increasing fluvial influence.

5.9. The modern lagoon

The short cores TR1 and TR2 consist of brown clayey silt (75.7% silt and 24.3% clay) at the base and dark clay and silt at the top (58.3% silt and 41.7% clay).

The GMD of texture at the base between 80 and 20 cm is 18 μm. X-ray diffraction at 50 cm depth shows significant quartz, moderate calcite, Mg-calcite, albite, gypsum, very minor halite, minor clinochlore and muscovite. The lowermost brown clayey silt contains little fauna and has low carbonate content (25%) in comparison with the upper part.

The biofacies (mostly foraminifera, ostracoda, and shell debris) seems to be largely reworked fauna. The lower brown deposit was formed during rapid sea-level fall and originated mostly from mainland deposition (Fig. 4a).

The GMD of the upper dark clay and silt is 8 μm. The XRD mineralogy at 15 cm depth indicates moderate quartz, Mg-calcite, minor to moderate calcite, minor albite, muscovite, clinochlore and very minor halite. The organic and carbonate contents are 5% and 32% respectively.

The dark clay and silt contain bivalves, mostly Cerastoderma and *Dreissena*, Gastropoda, foraminifera (*Ammonia beccarii*), Ostracoda (*Cyprideis*) and shell fragments without any dominant species. It also contains abundant seeds, mostly *Chenopodiaceae* and few gyrogonites.

Only the upper centimeters of these two cores have been analyzed for palynology. They serve to characterize the palynomorphs of the modern lagoon as the samples are taken from the interphase between water and sediment. The salt marsh is strongly represented by higher values of A–C than in the TM core. *Ruppia*, a submerged plant of brackish waters, has extremely large pollen percentages. Some foraminiferal linings have been encountered, while the dinocysts remain discrete and are alternatively dominated by *Lingulodinium machaerophorum*, or by *Impagidinium caspienense*. Hardly any Pteridophytic spores are observed. On the whole the core top couple of centimeters reflect a fresh environment without river influence, and with no direct equivalent in the TM core.

It is likely that the lowermost brown clayey silt between 80 and 20 cm depth were deposited during that last period of low water level between 1929 and 1977, and that the upper dark clay and silt were formed in water due to the post-1977 sea-level rise.

6. Discussion

The interpretation of the data from the TM core in terms of sea-level change is discussed below and summarized in Fig. 9. The total subsidence rate is around 10 m according to Allen et al. (2002).

6.1. Late Pleistocene fluctuation

The oldest facies recovered, at the base of the core at an absolute depth of around 53 m BOL and with one date on ostracoda at around 20,120 cal yr BP, shows marine deposits with few fossils. These gray to brownish laminated deposits differ considerably from overlying sediment both by biofacies, structure, geochemistry and color. High concentrations of major and trace elements (Kakroodi, 2012) such as Ti and Fe seem to point to a provenance from loessic sediments. According to Frechen et al. (2009), a period of increased loess accumulation corresponds with the Last Glacial Maximum and the Late Glacial, as suggested by IRSL ages ranging from 20.7 ± 1.9 to 15.2 ± 1.4 ka. The loessic sediments were fluvially reworked and deposited in the CS at a shallow depth. A deep core of the south basin (Pierret et al., 2012) also has recorded this loess influence at that time.

A few Pleistocene *Elphidium* foraminifera occur at the base of the core, and *Ammonia beccarii* is totally absent. According to Boomer et al. (2005), in the CS, foraminifera have only been recorded from sites shallower than 50 m of water. The main biota within these sediments are the ostracods *Leptocythere bacuana*, *Bacuniella dorsoarcuata* and *Eucythere*

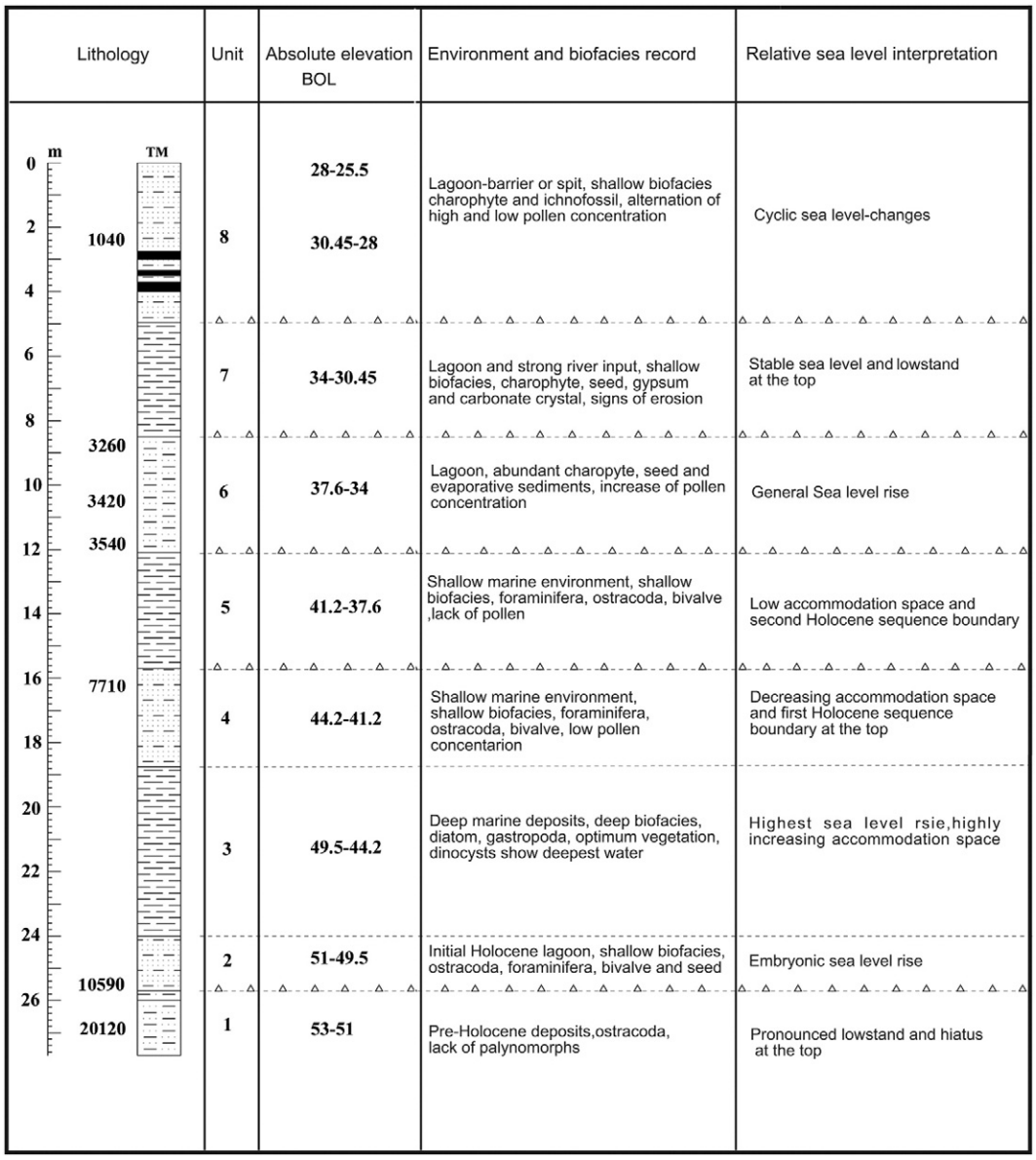

Fig. 9. Sea-level interpretation of the Late Pleistocene to Holocene time associated with biofacies and sedimentology data from core TM. The lines with triangles indicate the sequence boundaries.

naphtatscholana which disappear in the Holocene sedimentary record. Diatoms are absent in these sediments, possibly because silica is dissolved in the deeper part of the CS (Jelinowska et al., 1998). No palynomorphs were preserved due to the oxidized nature of the deposit.

At the top of Unit 1 between 26 and 25.7 m depth, the homogeneous nature of this material and the mottling suggest temporary emergence, oxidation and soil formation during a lowstand. Dissolution might also explain the low concentration of fauna and flora at the base. The exact sea-level at this time cannot be established from the available data, but using the absolute elevation of the hiatus it should be at least lower than 50 m BOL.

In general, a good correspondence is found between our data and previously published data. The reddish deposits at the bottom correlate well with similar Late Glacial brownish to reddish sediments which are also reported by Chalié et al. (1997) and Jelinowska et al. (1998) from deeper parts of the Caspian Sea Basin, and by Kroonenberg et al. (2010) from the Kura delta in Azerbaijan. They might correspond to the coeval so-called 'chocolate clays' in the North-Caspian Basin (Kroonenberg et al., 1997; Maev and Chepalyga, 2002; Badyukova, 2007) (see below). The record is not deep enough to confirm or refute correlation of these sediments with the Late Glacial–Early Khvalynian transgression. On the other hand, the major hiatus at the top of Unit 1 corresponds well with the well-known Early Holocene–Mangyshlak regression reported elsewhere in the Caspian (down to 92 m BOL, Kroonenberg et al., 2010).

Late Glacial reddish sediments such as those recovered in our core and elsewhere in the Caspian have also been found in the Black Sea in several places (Bahr et al., 2005; Major et al., 2006). According to Bahr et al. (2005) and Major et al. (2006), between around 18 and 15 cal yr BP a series of red layers have been deposited in the Black Sea assuming a water overflow from the Caspian Sea during the Early Khvalynian transgression probably due to melt water from the Scandinavian ice sheet, though the precise timing of these events is still ambiguous. Our only radiocarbon date at the bottom of the core indicates an age around 17,300 uncal yr PB.

From the TM core, it is not possible to say if the lowstand experienced between Units 1 and 2, related to the regional Mangyshlak lowstand, corresponds or not to the Younger Dryas. While the YD has been identified in the terrestrial environment in a deep core form the

south basin (Pierret et al., 2012), it is so far still unclear how this translated into the marine environment and into any related sea-level changes due to the overpowering influence of the re-organization of the regional paleo-hydrography.

6.2. Holocene sea-level changes

Fig. 9 summarizes sea-level interpretation based on multi-proxy data. Lagoonal silt and clay recovered at an absolute elevation of around 51 m BOL overlain by fine sand in Unit 2 suggest that the lowstand at the top of Unit 1 (expressed by a hiatus) was followed around 10,590 cal yr BP by gradual CSL rise. Charophytes appeared for a short time in the initial lagoonal system, showing a transition of fresh water to at least brackish water with 5 g/l. However, they disappear rapidly again due to increasing accommodation space. Sea-level rise continues into Unit 3, the most marine unit of the whole core. It is striking that whereas gastropoda, dinocysts and ostracods indicate a deeper water -environment, the massive brackish and fresh diatoms in this unit and the oxygen isotopes give typical fresh water values. A vegetation optimum indicates optimal precipitation on the nearby Alborz Mountains. All these suggest that the highstand evidenced in Unit 3 was the result of the influx of a large volume of fresh water, most likely meltwater, between around 10,590 and 7710 cal yr BP. Based on a calculated sedimentation rate of around 3.12 mm/y, the highstand occurred between 10,000 and 8400 cal yr BP.

This continuous sea-level rise from around 10,590 to around 8400 cal yr BP with a minimum value of oxygen isotope suggests a higher input of fresh water. This continuous sea-level rise between 10,590 and around 8400 cal yr BP in the lagoon systems which peaked in Unit 3 might synchronize with the 8200 cal yr BP event (Kobashi et al., 2007), a period of cool and dry climate and therefore less evaporation. A regional sea-level rise has also been reported during the maximum sea-level in the TM core (Bahr et al., 2005, 2008; Major et al., 2006; Frigola et al., 2007; Badertscher et al., 2011). Some authors have suggested a hydrological source from the eastern part of the CS which is inactive now (Boomer et al., 2000; Leroy et al., 2013). It can also be considered melted snows from Volga's drainage basin or in the Albourz mountain range surrounded by the CS which one of the glacier still surviving in Alamkoh.

In Unit 4 recovered at around 44.2 m BOL, diatom values decrease strongly, and benthic foraminifera start to dominate. A major shift of oxygen isotope values to more positive values takes place, eventually abutting into the first Holocene sequence boundary dated on foraminifera around 7710 cal yr BP, located at ~42 m BOL. Such a great lowstand could only be interpreted by assuming a major decrease of river inflow into the basin and much more evaporation. The progressively increased scarcity of pollen is probably related to temporary emergence and oxidation during this lowstand.

A subsequent slight sea-level rise led to a shallow marine environment with low abundance of fauna in Unit 5. According to Rychagov (1997) sea-level rose rapidly after the 7248 ± 50 uncal yr BP lowstand and reached −20 m BOL (Fig. 2); However, our data, especially the biofacies and presence of evaporites suggest only gradual sea-level rise, continuing shallow water conditions, ending in another lowstand at the top of this unit. The absence of pollen in this unit probably reflects oxidation during this lowstand.

The well-developed lagoonal environment at around 37 m BOL evidenced in Unit 6 recovered at around 37.6 m BOL shows that, after the second Holocene lowstand, CSL started to rise again. A significant change of biofacies, mostly Charophyte numbers, organic matter and carbonate contents reflect a major change in the Caspian Sea, again characterized both by sea-level rise and a highstand tract with no subaerial facies. During increasing accommodation space, lagoons shifted landwards, depositing the dark clay facies, whereas during highstand shallow-water carbonate–gypsum evaporitic facies formed at the top of the lagoonal facies. This parasequence pattern occurs when prolonged relative sea-level rise and low terrigenous input occur; otherwise lagoonal facies are exposed and infilled by fluvial sediment. The alternation of evaporative sediment and lagoonal facies are the main depositional patterns of the mid-Holocene deposits showing rapid sea-level rise and repeated highstands. The 3 and 12-cm thick shell beds with entire and broken valves in Unit 6 record at least two storm events. Radiocarbon dates of 3540, 3420 and 3260 cal yr BP have been obtained from Gastropoda from this unit at 10.1 and 8.9 m depths, in harmony with the period of sea-level rise between 5000 and ~ 2300 cal yr BP obtained by Kroonenberg et al. (2008), Hoogendoorn et al. (2010) and Kakroodi et al. (2012).

In Unit 7 recovered at around 34 m BOL, a shallow lagoonal environment with few Caspian biota reflects no major change of sea-level; however the lagoon is strongly affected by more river input. As a whole, the sea-level was stable and at least no major evidence of sea-level rise and fall is found in this unit.

Unit 8 recovered at around 30.45 m BOL shows rapid alternations of lagoonal dark clayey silts and barrier like terrigenous facies characterized by reworked fauna and ichnofossils (Fig. 9), suggesting rapid sea-level change close to the paleoshoreline. Along shallow coasts, even small relative sea-level changes would result in emergence and submergence of large marginal portions of the basin, as also observed between 1929 and 1995 in the CS (Kakroodi et al., 2012). This is corroborated by the presence of Trichoptera ichnofossils, the activity of which is known to be limited to the sea–land interface (shoreline). Temporary exposure is also suggested by the brown to reddish colored sand at the top of dusky clayey silt. The record shows that at least five late Holocene sea-level cycles have occurred after 3260 cal yr BP. From these cycles, two major periods of cooling phases occurred in the 2600–2300 cal yr BP highstand and Little Ice Age (Kroonenberg et al., 2007; Leroy et al., 2011; Kakroodi et al., 2012, 2014a,b) with a strong impact on the Caspian Sea-level.

7. Conclusions

The Caspian Sea-level history since the Late Pleistocene was reconstructed using a multi-disciplinary approach. A nearly continuous record of the Late Pleistocene and Holocene deposition was subdivided into eight units and each unit was identified by biostratigraphic, sedimentological, geochemical, geochronological and palynological (pollen, NPPs and dinocysts) data. Sea-level changes in the CS can be subdivided into six periods as follows:

(1) The Late Pleistocene sediments differ strongly from the early Holocene sediments in Pleistocene ostracoda, and lack of palynomorphs. The Black Sea and the Caspian Sea probably share their history at this time as a similar red sediment layer is reported at both basins.
(2) At the boundary of Pleistocene and Holocene, Caspian Sea-level experienced a deep lowstand at least lower than 53 m BOL.
(3) Caspian Sea-level started to rise, as evidenced by the formation of lagoonal sediments at around 10,590 cal yr BP; the coast shifted landward without any lowstand record. This indicates a typical sea-level rise associated with charophyte and a well developed lagoon–barrier system.
(4) The Caspian Sea was at its maximum level between around 10,590 and 8400 cal yr BP, as evidenced by diatoms, optimum vegetation, dinocysts of open seas, and the most negative oxygen isotope value of the whole core. Due to the high accommodation space a biota transition from lagoonal environment (charophyte) to deeper part (diatom) occurred.
(5) The first Holocene lowstand, around 41 m BOL, occurred at 7710 cal yr BP, evidenced by a low concentration of palynomorphs, biofacies change (from diatom to foraminifera) and a positive oxygen isotope ratio. A subsequent moderate sea-level rise led to shallow marine environment and ended

with another lowstand at 41.2 m BOL.

(6) The Mid-Holocene started again with a lagoonal environment, showing a major change in palynology, biofacies (mainly Charophyte) and carbonate content characterized by two parasequence sets. Subsequent Caspian Sea-level rise led to the formation of another highstand facies on top of the lagoonal facies.

(7) The Late Holocene dynamics is characterized by sea-level fluctuations with alternating emergence and submergence associated with ichnofossils and Charophyte respectively. At least five Holocene sea-level cycles have been identified commencing at 3260 cal yr BP. This indicates different behaviors of the Caspian Sea than those of the early and midHolocene sea-level change.

In conclusion, during the Late Pleistocene and the Holocene the south-east coast of the CS has experienced repeated, vast and rapid changes from fully marine environments to shallow lagoonal ones with deep impacts on water salinity and vegetation, and the displacements of large volumes of sediment.

Acknowledgments

This project was funded by the Oceanography Institute and Cultural Heritage Tourism Organization of Mazandaran. Most laboratory analyses were carried out at international oceanography laboratories in Tehran and at the Nowshahr station (INIO). We would like to thank Mr. Taheri and Dr. Wesselingh for their help in identifying Caspian Sea fauna. We thank Mrs. Habibi for her assistance with measurements of organic matter and carbonate content. Finally, my brothers, Ghahraman and Abdollah, provided me with all the facilities that I needed in the fieldwork. M. Turner (Brunel University) has kindly revised the language of the manuscript. This publication is a contribution to the INQUA QuickLakeH project (no. 1227).

References

Allen, M.B., Jones, S., Ismail-Zadeh, A., Simmons, M., Anderson, L., 2002. Onset of subduction as the cause of rapid Pliocene–Quaternary subsidence in the South Caspian basin. Geology 30, 775–778.

Arpe, K., Leroy, S.A.G., Lahijani, H., Khan, V., 2012. Impact of the European Russia drought in 2010 on the Caspian Sea-level. Hydrology and Earth System Sciences 16, 19–27.

Badertscher, S., Fleitmann, D., Cheng, H., Edwards, R.L., Göktürk, O.M., Zumbühl, A., Leuenberger, M., Tüysüz, O., 2011. Pleistocene water intrusions from the Mediterranean and Caspian seas into the Black Sea. Nature 4, 236–239.

Badyukova, E.N., 2007. Age of Khvalynian Transgressions in the Caspian Sea Region, *Okeanologiya*. Oceanology (English Translational) 47 (no. 3), 432–438 (vol. 47, no. 3, pp. 400–405).

Bahr, A., Lamy, F., Arz, H.W., Kuhlmann, H., Wefer, G., 2005. Late glacial to Holocene climate and sedimentation history in the NW Black Sea. Marine Geology 214 (4), 309–322.

Bahr, A., Lamy, F., Arz, H.W., Major, C., Kwiecien, O., Wefer, G., 2008. Abrupt changes of temperature and water chemistry in the Late Pleistocene and early Holocene Black Sea. Geochemistry, Geophysics, Geosystems 9 (1), Q01004.

Behre, K.-E., 1981. The interpretation of anthropogenic indicators in pollen diagrams. Pollen et Spores 23, 225–245.

Bennett, K., 2007. Documentation for Psimpoll and Pscomb. http://www.chrono.qub.ac.uk/psimpoll/psimpoll.html (last accessed on 31 Aug. 2010).

Birshtein, Y.A., Romanova, N.N., 1968. Order Amphipoda. In: Birshtein, Y.A., Vinogradov, L.G., Kondakov, N.N., Astakhova, M.S., Romanova, N.N. (Eds.), Atlas of Invertebrates of the Caspian Sea. Pishchevaya Promyshlennost, Moscow, pp. 241–289 (in Russian).

Boomer, I., Aladin, N., Plotnikov, I., Whatley, R., 2000. The palaeolimnology of the Aral Sea: a review. Quaternary Science Reviews 19, 1259–1278.

Boomer, I., von Grafenstein, U., Guichard, F., Bieda, S., 2005. Modern and Holocene sublittoral ostracod assemblages (Crustacea) from the Caspian Sea: a unique brackish, deep-water environment. Palaeogeography, Palaeoclimatology, Palaeoecology 225, 173–186.

Chalié, F., Escudié, A.-S., Badaut-Trauth, D., Blanc, G., Blanc-Valleron, M.-M., Brigault, S., Desprairies, A., Ferronsky, V.I., Giannesini, P.-J., Gibert, E., Guichard, F., Jelinowska, A., Massault, M., Mélières, F., Tribovillard, N., Tucholka, P., Gasse, F., 1997. The glacial–postglacial transition in the southern Caspian Sea. Comptes Rendus de l'Académie des Sciences de Paris 324 (IIa), 309–316.

Church, J.A., Clark, P.U., Cazenave, A., Gregory, J.M., Jevrejeva, S., Levermann, A., Merrifield, M.A., Milne, G.A., Nerem, R.S., Nunn, P.D., Payne, A.J., Pfeffer, W.T., Stammer, D., Unnikrishnan, A.S., 2013. Sea-level change. In: Stocker, T.F., Qin, D., Plattner, G.-K., Tignor, M., Allen, S.K., Boschung, J., Nauels, A., Xia, Y., Bex, V., Midgley, P.M. (Eds.), Climate Change 2013: The Physical Science Basis. Contribution of Working Group I to the Fifth Assessment Report of the Intergovernmental Panel on Climate Change. Cambridge University Press, Cambridge, United Kingdom and New York, NY, USA.

Dolukhanov, P.M., Chepalyga, A.L., Lavrentiev, N.V., 2010. The Khvalynian transgressions and early human settlement in the Caspian basin. Quaternary International 225, 152–159.

Ferronsky, V.I., Brezgunov, V.S., Vlasova, L.S., Polyakov, V.A., Froehlich, K., Rozansky, K., 2003. Investigation of water-exchange processes in the Caspian Sea on the basis of isotopic and oceanographic data. Water Resources 30 (1), 10–22.

Frechen, M., Kehl, M., Rolf, C., Sarvati, R., Skowrone, A., 2009. Loess chronology of the Caspian Lowland in Northern Iran. Quaternary International 198, 220–233.

Frigola, A., Moreno, A., Cacho, I., Canals, M., Sierro, F.J., Flores, J.A., Grimalt, J.O., Hodell, D.A., Curtis, J.H., 2007. Holocene climate variability in the western Mediterranean region from a deepwater sediment record. Paleoceanography 22, PA2209.

Hoogendoorn, R.M., Boels, J.F., Kroonenberg, S.B., Simmons, M.D., Aliyeva, E., Babazadeh, A.D., Huseynov, D., 2005. Development of the Kura delta, Azerbaijan; a record of Holocene Caspian sea-level changes. Marine Geology 222–223, 359–380.

Hoogendoorn, R.M., Levchenko, O., Missiaen, T., Lychagin, M., Richards, K., Gorbunov, A., Kasimov, N., Kroonenberg, S.B., 2010. High resolution seismic stratigraphy of the modern Volga delta, Russia. International Conference. The Caspian Region, Moscow, pp. 32–37.

Hustedt, F., 1930. In: Die süsswasser-Flora Mitteleuropas Heft (Ed.), Bacillariophyta (Diatomeae). 10, pp. 1–466.

Inan, S., Yalcin, M.N., Guliyev, I.S., Kuliev, K., Feizullayev, A.A., 1997. Deep petroleum occurrences in the Lower Kura depression, South Caspian Basin, Azerbaijan: an organic chemical and basin modeling study. Marine and Petroleum Geology 14, 731–762.

Jackson, J., Priestley, K., Allen, M., Berberian, M., 2002. Active tectonic of the south Caspian basin. Geophysical Journal International 148, 214–245.

Jelinowska, A., Tucholka, P., Guichard, F., Lefèvre, I., Badaut-Trauth, D., Chalié, F., Gasse, F., Tribovillard, N., Desprairies, A., 1998. Mineral magnetic study of late quaternary South Caspian Sea sediments, palaeoenvironmental implications. Geophysical Journal International +3, 499–509.

Kakroodi, 2012. Rapid Caspian Sea-level Change and Its Impact on Iranian Coasts. PhD thesis. Delft University of Technology.

Kakroodi, A.A., Kroonenberg, S.B., Hoogendoorn, R.M., Mohammadkhani, H., Yamani, M., Ghasssemi, M.R., Lahijani, H.A.K., 2012. Rapid Holocene sea-level changes along the Iranian Caspian coast. Quaternary International 263 (93H.A).

Kakroodi, A.A., Kroonenberg, S.B., Naderi Beni, A., Noehgar, N., 2014a. Short- and long-term development of the Miankaleh Spit, Southeast Caspian Sea, Iran. Journal of Coastal Research 30 (6), 1236–1242.

Kakroodi, A.A., Kroonenberg, S.B., Goorabi, A., Yamani, M., 2014b. Shoreline response to rapid 20th century sea-level change along the Iranian Caspian coast. Journal of Coastal Research 30 (6), 1243–1250.

Kaplin, P.A., Selivanov, A.O., 1995. Recent coastal evolution of the Caspian Sea as a natural model for coastal response to the possible acceleration of global sea-level rise. Marine Geology 124, 161–175.

Karayeva, N.I., Makarova, I.V., 1973. Specific features of the Caspian Sea diatom flora. Marine Biology 21, 269–275.

Karpinsky, M.G., 2005. Biodiversity. Hdb Env Chem vol. 5. Springer-Verlag, Berlin Heidelberg, pp. 159–173 (Part P).

Kazanci, N., Gulbabazadeh, T., 2013. Sefidrud delta and Quaternary evolution of the southern Caspian lowland. Marine and Petroleum Geology 44, 120–139.

Kazancı, N., Gulbabazadeh, T., Leroy, S.A.G., Ileri, O., 2004. Sedimentary and environmental characteristics of the Gilan–Mazenderan plain, northern Iran: influence of long- and short-term Caspian water level fluctuations on geomorphology. Journal of Marine Systems 46 (1–4), 145–168.

Kobashi, T., Severinghaus, J.P., Brook, E.J., Barnola, J.-M., Grachev, A.M., 2007. Precise timing and characterization of abrupt climate change 8200 years ago from air trapped in polar ice. Quaternary Science Reviews 26, 1212–1222.

Kroonenberg, S.B., Rusakov, G.V., Svitoch, A.A., 1997. The wandering of the Volga delta: a response to rapid Caspian Sea-level changes. Sedimentary Geology 107, 189–209.

Kroonenberg, S.B., Badyukova, E.N., Storms, J.E.A., Ignatov, E.I., Kasimov, N.S., 2000. A full sea-level cycle in sixty-five years: barrier dynamics along Caspian shores. Sedimentary Geology 134, 257–274.

Kroonenberg, S.B., Abdurakhmanov, G.M., Badyukovac, K., van der Borg, E.N., Kalashnikov, A., Kasimov, N.S., Rychagov, G.I., Svitoch, A.A., Vonhof, H.B., Wesselingh, F.P., 2007. Solar-forced 2600 BP and Little Ice Age highstands of the Caspian Sea. Quaternary International 173–174, 137–143.

Kroonenberg, S.B., Kasimov, N.S., Lychagin, M.Yu., 2008. The Caspian Sea, a natural laboratory for sea-level change. Geography, Environment, Sustainability 1 (1), 22–37.

Kroonenberg, S.B., Aliyeva, E., de Baptist, M., Hoogendoorn, R.M., Huseynov, D., Huseynov, R., Kasimov, N.S., Lychagin, M., Missiaen, T., De Mol, L., Popescu, S., Suc, J.P., 2010. Pleistocene connection and Holocene separation of the Caspian and 1031 Black Seas: data from the modern Kura delta, Azerbaijan. International 1032 Conference. The Caspian Region, Moscow, pp. 17–20.

Kuzmin, Y.V., Nevesskaya, L.A., Krivonogov, S.K., Burr, G.S., 2007. Apparent ^{14}C ages of the 'pre-bomb' shells and correction values (R, ΔR) for Caspian and Aral Seas (Central Asia). Nuclear Instruments and Methods in Physics Research B 259, 463–466.

Lamb, A.L., Wilson, G.P., Leng, M.J., 2006. A review of coastal paleoclimate and relative sea reconstruction using $\partial^{13}C$ and C/N ratios in organic material. Earth Science Reviews 75, 29–57.

Leroy, S.A.G., Marret, F., Giralt, S., Bulatov, S.A., 2006. Natural and anthropogenic rapid changes in the Kara-Bogaz Gol over the last two centuries by palynological analyses. Quaternary International 150, 52–70.

Leroy, S.A.G., Marret, F., Gibert, E., Chalié, F., Reyss, J.-L., Arpe, K., 2007. River inflow and salinity changes in the Caspian Sea during the last 5500 years. Quaternary Science Reviews 26, 3359–3383.

Leroy, S.A.G., Warny, S., Lahijani, H., Piovano, E.L., Fanetti, D., Berger, A.R., 2010. The role of geosciences in the mitigation of natural disasters: five case studies. In: Beer, T. (Ed.), Geophysical Hazards: Minimising Risk, Maximising Awareness. Springer Science, in series International Year of Planet Earth, pp. 115–147 (Chap. 9).

Leroy, S.A.G., Lahijani, H.A.K., Djamali, M., Naqinezhad, A., Moghadam, M.V., Arpe, K., Shah-Hosseini, M., Hosseindoust, M., Miller, Ch.S., Tavakoli, V., Habibi, P., Naderi, M., 2011. Late Little Ice Age palaeoenvironmental records from the Anzali and Amirkola lagoons (south Caspian Sea): vegetation and sea level changes. Palaeogeogr. Palaeoclimatol. Palaeoecol. 302, 415–434.

Leroy, S.A.G., Kakroodi, A.A., Kroonenberg, S.B., Lahijani, H.A.K., Alimohammadian, H., Nigarov, A., 2013. Holocene vegetation history and sea level changes in the SE corner of the Caspian Sea: relevance to SW Asia climate. Quat. Sci. Rev. 70, 28–47.

Lewis, D.W., McConchie, D., 1994. Analytical Sedimentology. Chapman and Hall, New York (197 p.).

Maev, E.V., Chepalyga, A.L., 2002. The Caspian Sea. In: Velichko, A.A. (Ed.), Dynamics of Terrestrial Landscape Components and Closed Marine Basins of Northern Eurasia During the Last 130,000 Years, pp. 182–190.

Major, C.O., Goldstein, S.L., Ryan, W.B.F., Lericolais, G., Piotrowski, A.M., Hajdas, I., 2006. The co-evolution of Black Sea-level and composition through the last deglaciation and its paleoclimatic significance. Quaternary Science Reviews 25, 2031–2047.

Mangerud, J., Jakobsson, M., Alexanderson, H., Astakhov, V., Clarke, G.K.C., Henriksen, M., Hjort, C., Krinner, G., Lunkka, J.-P., Moller, P., Murray, A., Nikolskaya, O., Saarnisto, M., Svendsen, J.I., 2004. Ice-dammed lakes and rerouting of the drainage of northern Eurasia during the last glaciation. Quaternary Science Reviews 23, 1313–1332.

Mansimov, M., Aliyev, A., 1994. Reasons of Caspian Sea-level fluctuations and predictions for future. Azerbaijan International A1 (2.3), 48–49.

Marret, F., Leroy, S., Chalié, F., Gasse, F., 2004. New organic-walled dinoflagellate cysts from recent sediments of central Asian seas. Review of Palaeobotany and Palynology 129, 1–20.

Mertens, K.N., Ribeiro, S., Bouimetarhan, I., Caner, H., Combourieu-Nebout, N.Mertens, K.N., Ribeiro, S., Bouimetarhan, I., Caner, H., Combourieu-Nebout, N., Dale, B., de Vernal, A., Ellegaard, M., Filipova, M., Godhe, A., Grøsfjeld, K., Holzwarth, U., Kotthoff, U., Leroy, S., Londeix, L., Marret, F., Matsuoka, K., Mudie, P., Naudts, L., Peña-manjarrez, J., Persson, A., Popescu, S., Sangiorgi, F., van derMeer, M., Vink, A., Zonneveld, K., Vercauteren, D., Vlassenbroeck, J., Louwye, S., 2009. Process length variation in cysts of a dinoflagellate, *Lingulodinium machaerophorum*, in surface sediments investigating its potential as salinity proxy. Marine Micropaleontology 70, 54e69.

Mister, R., 2001. Draft Report of the UN INTER-Agency Flood Report of the Golestan, Iran. www.reliefweb.int/ochaunep/edr/IranGolestan.pdf.

Mudie, P.J., Leroy, S.A.G., Marret, F., Gerasimenko, N., Kholeif, S.E.A., Sapelko, T., Filipova-Marinova, M., 2011. Non-pollen palynomorphs: indicators of salinity and environmental change in the Caspian–Black Sea–Mediterranean Corridor. In: Buynevich, I., Yanko-Hombach, V., Gilbert, A.S., Martin, R.E. (Eds.), Geology and Geoarchaeology of the Black Sea Region: Beyond the Flood Hypothesis. Geological Society of America Special Paper 473, pp. 89–115. http://dx.doi.org/10.1130/2011.2473(07).

Nerem, R.S., Leuliette, E., Cazenave, A., 2006. Present-day sea-level change: a review. Comptes Rendus Geoscience 338, 1077–1083.

Pierret, M.C., Chabaux, F., Leroy, S.A.G., Causse, C., 2012. A record of Late Quaternary continental weathering in the sediment of the Caspian Sea: evidence from U–Th, Sr isotopes, trace element and palynological data. Quaternary Science Reviews 51, 40–55.

Reimer, P.J., Baillie, M.G.L., Bard, E., Bayliss, A., Beck, J.W., Blackwell, P.G., Bronk Ramsey, C., Buck, C.E., Burr, G.S., Edwards, R.L., Friedrich, M., Grootes, P.M., Guilderson, T.P., Hajdas, I., Heaton, T.J., Hogg, A.G., Hughen, K.A., Kaiser, K.F., Kromer, B., McCormac, F.G., Manning, S.W., Reimer, R.W., Richards, D.A., Southon, J.R., Talamo, S., Turney, C.S.M., van der Plicht, J., Weyhenmeyer, C.E., 2009. Calib Radiocarbon Calibration. http://calib.qub.ac.uk/calib/download.

Rodionov, S.N., 1994. Global and Regional Climate Interaction: The Caspian Sea Experience. Kluwer, Dordrecht (254 pp.).

Rychagov, G.I., 1977. The Pleistocene History of the Caspian Sea. D.Sc. Thesis, Moscow State University (252 pp. Autoreferate 62 pp. (in Russian)).

Rychagov, G.L., 1997. Holocene oscillation of the Caspian Sea, and forecast based on the Caspian Sea and forecast based on paleogeographical reconstructions. Quaternary International 41 (42), 167–172.

Sidorchuk, A.Y.U., Panin, A.V., Borisova, O.K., 2009. Morphology of river channels and surface runoff in the Volga River basin (East European Plain) during the Late Glacial period. Geomorphology 113, 137–157.

Soulié-Märche, I., 2008. Charophytes, indicators for low salinity phases in North African sebkhet. Journal of African Earth Sciences 51, 69–76.

Svitoch, A.A., 2009. Khvalynian transgression of the Caspian sea was not a result of water overflow from the Siberian Proglacial lake, nor a prototype of the Noachian flood. Quaternary International 197, 115–125.

Svitoch, A.A., Badyukova, E.N., Kroonenberg, S.B., Parunin, O.B., Vonhof, H.V., 2006. Radiocarbon dating of mollusc shells from marine deposits from the Caspian shore in Dagestan. Bulletin of the Moscow State University 53, 13–21 (in Russian).

Tiffany, L.H., Britton, M.E., 1952. Algae of Illinois. The University of Chicago Press, Chicago, pp. 1–407.

Varushchenko, S.I., Varushchenko, A.N., Klige, R.K., 1987. Regime Change of the Caspian Sea and Enclosed Water Bodies in Paleotime. Nauka, Moscow (240 pp. (in Russian)).